# Calcium-dependent copper redistributions in neuronal cells revealed by a fluorescent copper sensor and X-ray fluorescence microscopy

Sheel C. Dodani[a,1], Dylan W. Domaille[a,1], Christine I. Nam[a,b,1], Evan W. Miller[a], Lydia A. Finney[c], Stefan Vogt[c], and Christopher J. Chang[a,b,2]

[a]Department of Chemistry, University of California, Berkeley, CA 94720; [b]Howard Hughes Medical Institute, University of California, Berkeley, CA 94720; and [c]X-Ray Sciences Division and Biosciences Division, Argonne National Laboratory, 9700 South Cass Avenue, Argonne, IL 60439

Edited* by Harry B. Gray, California Institute of Technology, Pasadena, CA, and approved February 23, 2011 (received for review July 9, 2010)

**Dynamic fluxes of s-block metals like potassium, sodium, and calcium are of broad importance in cell signaling. In contrast, the concept of mobile transition metals triggered by cell activation remains insufficiently explored, in large part because metals like copper and iron are typically studied as static cellular nutrients and there are a lack of direct, selective methods for monitoring their distributions in living cells. To help meet this need, we now report Coppersensor-3 (CS3), a bright small-molecule fluorescent probe that offers the unique capability to image labile copper pools in living cells at endogenous, basal levels. We use this chemical tool in conjunction with synchotron-based microprobe X-ray fluorescence microscopy (XRFM) to discover that neuronal cells move significant pools of copper from their cell bodies to peripheral processes upon their activation. Moreover, further CS3 and XRFM imaging experiments show that these dynamic copper redistributions are dependent on calcium release, establishing a link between mobile copper and major cell signaling pathways. By providing a small-molecule fluorophore that is selective and sensitive enough to image labile copper pools in living cells under basal conditions, CS3 opens opportunities for discovering and elucidating functions of copper in living systems.**

fluorescent sensor | molecular imaging | mobile metals | transition metal signaling

Metals are essential components of all living cells, and in many cases cells trigger and utilize dynamic metal movements for signaling purposes. Such processes are well established for alkali and alkaline earth metals like potassium, sodium, and calcium (1–3) but not for transition metals like copper and iron, which are traditionally studied for their roles as static cofactors in enzymes (4–6). We have initiated a program aimed at exploring the concept of mobile transition metals and their contributions to cell physiology and pathology, and in this context, brain neurons offer an attractive model for this purpose owing to their widespread use of potassium and sodium ion channels and calcium release for signaling events (7), as well as a high requirement for copper and iron to meet their steep oxidative demand (8–12). Indeed, the brain needs much higher levels of copper compared to other parts of the body under normal physiological conditions (9, 12), but at the same time mishandling of neuronal copper stores and subsequent oxidative stress and damage events are connected to a variety of neurodegenerative ailments, including Menkes and Wilson's diseases (13, 14), Alzheimer's disease (15–17), familial amyotrophic lateral sclerosis (18, 19), and prion-mediated encephalopathies (20, 21). Previous work hints at the importance of exchangeable copper in neurophysiology, including observations of $^{64}$Cu efflux from stimulated neurons (22, 23), export of Cu from isolated synaptosomes (24), and elevated susceptibility of neurons to excitotoxic insult with copper chelation (25), but none of these reports show direct, live-cell monitoring of spatial copper distributions during various stages of neural activity.

Along these lines, molecular imaging with copper-responsive fluorescent sensors offers a potentially powerful methodology for interrogating its cell biology by allowing the specific tracking of copper pools in living cells with spatial and temporal resolution (12, 26–32). In this regard, analogous tools have revolutionized the study of calcium in a variety of biological settings (1) and hold promise for interrogating other cellular metals (26). However, fluorescence-based sensing of $Cu^+$, the oxidation state stabilized in reducing cytosolic environments, presents several additional challenges that make it more difficult to detect compared to other abundant metal ions in cells (e.g., $Na^+$, $K^+$, $Ca^{2+}$, $Mg^{2+}$, $Zn^{2+}$). The most prominent of these challenges include (*i*) redox specificity over $Cu^{2+}$, the other major oxidation state for biological copper, (*ii*) the propensity for $Cu^+$ in water to disproportionate to $Cu^{2+}$ and Cu metal, and (*iii*) the ability of $Cu^+$ to quench fluorescence by electron and/or energy transfer. Indeed, of the growing number of reported strategies for fluorescence copper detection (12, 26), only three synthetic sensors, CTAP-1 (29), CS1 (30, 31), and RCS1 (32), and two protein-based sensors (33, 34) have been validated for live-cell imaging with $Cu^+$. Moreover, the relatively low quantum efficiencies of the first-generation synthetic reagents ($\Phi \leq 0.14$ in $Cu^+$-bound forms) have limited their use to date for cellular imaging under conditions of prolonged copper overload or depletion.

Here, we present the synthesis, properties, and applications of Coppersensor-3 (CS3), a bright fluorescent sensor that now offers the unique ability to detect labile copper pools at basal, endogenous levels in living cells. This BODIPY-based probe features high selectivity over competing cellular metal ions, including redox differentiation between $Cu^+$ and $Cu^{2+}$, visible wavelength excitation and emission profiles, and a 75-fold fluorescence turn-on response with high quantum efficiency ($\Phi = 0.40$) for $Cu^+$ detection. By using this chemical tool in conjunction with synchotron-based microprobe X-ray fluorescence microscopy (XRFM) in a combined imaging study, an approach that has been successfully employed for monitoring resting copper distributions in mammalian cells (29), we have discovered that neuronal cells trigger a marked translocation of copper pools from their cell bodies to extended outer processes when activated by depolarization. Moreover, additional CS3 and microprobe XRFM studies show that these dynamic copper movements are dependent on the

Author contributions: C.J.C. designed research; S.C.D., D.W.D., C.I.N., and E.W.M. performed research; S.C.D., D.W.D., C.I.N., L.A.F., and S.V. contributed new reagents/analytic tools; S.C.D., D.W.D., C.I.N., E.W.M., L.A.F., S.V., and C.J.C. analyzed data; and S.C.D., D.W.D., and C.J.C. wrote the paper.

The authors declare no conflict of interest.

*This Direct Submission article had a prearranged editor.

[1]S.C.D., D.W.D., and C.I.N. contributed equally to this work.

[2]To whom correspondence should be addressed. E-mail chrischang@berkeley.edu.

This article contains supporting information online at www.pnas.org/lookup/suppl/doi:10.1073/pnas.1009932108/-/DCSupplemental.

release of calcium, establishing a link between mobile copper and major cell signaling pathways. The combined advances in optical brightness and turn-on response for CS3 afford a host of opportunities for studying the cell biology of copper by providing the ability to visualize labile copper pools in living cells under basal and stimulated conditions.

## Results and Discussion

**Design, Synthesis, and Spectroscopic Evaluation of Coppersensor-3 (CS3), a Bright Fluorophore for Selective Cu(I) Detection.** We previously reported Coppersensor-1 (CS1), a first-generation, selective turn-on fluorescent sensor for aqueous $Cu^+$ with visible excitation and emission profiles, and demonstrated its utility for live-cell imaging (30). This reporter shows good selectivity for $Cu^+$ over other cellular metal ions at physiologically relevant concentrations, a robust 10-fold fluorescence enhancement upon $Cu^+$ complexation, and allows for the visualization of $Cu^+$ in live mammalian cells under conditions of acute copper overload. However, attempts to use CS1 to interrogate the dynamics of endogenous cellular copper pools at basal levels were limited by the relatively low quantum yield of the CS1:$Cu^+$ complex ($\Phi = 0.13$). Seeking to maintain high $Cu^+$ specificity while improving optical brightness values and turn-on responses, we reasoned that increasing electron density on the fluorophore reporter would favor a greater turn-on enhancement through a brighter $Cu^+$-dye complex. Nagano's laboratory has previously shown that substitution of fluoro substituents with methoxy groups on the boron center of BODIPY fluorophores offers a practical strategy for tuning electronic properties of these fluorescent dyes (35). Fig. 1 details the synthetic route to Coppersensor-3 (CS3) based on these design considerations.

Spectroscopic analysis of apo CS3 in 20 mM HEPES buffered to pH 7 reveals one major peak in the visible region at 550 nm ($\varepsilon = 3.1 \times 10^4$ $cm^{-1}$ $M^{-1}$) with a shoulder at 511 nm. Maximal emission occurs at 560 nm with weak fluorescence ($\Phi = 0.007$). Addition of $Cu^+$ leads to a blue shift in the absorption band to 540 nm ($\varepsilon = 4.6 \times 10^4$ $cm^{-1}$ $M^{-1}$) and a large 75-fold increase in fluorescence intensity ($\Phi = 0.40$), with a corresponding hypsochromic shift in emission maximum to 548 nm (Fig. 2*A*). These values represent a significant improvement over the first-generation CS1 dye ($Cu^+$-bound $\Phi = 0.13$, 10-fold turn-on response) that has implications for its practical utility in cell imaging experiments (*vide infra*). Binding analysis using the method of continuous variations (Job's plot) indicates that a 1:1 $Cu^+$:dye complex is responsible for the turn-on fluorescence response observed for CS3 (*SI Text*). The apparent dissociation constant for the CS3:$Cu^+$ complex is $8.9(3) \times 10^{-14}$ M in HEPES buffer at pH 7 (*SI Text*).

CS3 exhibits high selectivity for $Cu^+$, even in the presence of physiologically relevant concentrations of competing metal ions (Fig. 2*B*). The fluorescence response of CS3 to $Cu^+$ is not affected by the presence of 2 mM $Ca^{2+}$, $Mg^{2+}$, and $Zn^{2+}$, nor do these metal ions cause increases in the fluorescence signal. Moreover, other biologically abundant transition metal ions (50 μM $Co^{2+}$, $Fe^{2+}$, $Mn^{2+}$, or $Ni^{2+}$) do not trigger false positives, nor do they interfere with $Cu^+$-induced fluorescence enhancements for CS3. More importantly, 50 μM $Cu^{2+}$ neither causes a fluorescence increase nor hinders the response of CS3 to $Cu^+$, indicating that CS3 maintains oxidation state specificity for $Cu^+$ over $Cu^{2+}$. Finally, owing to the thioether groups in the sensor we have included a panel of trace soft heavy metal ions for selectivity studies, including $Hg^{2+}$, $Ag^+$, $Tl^+$, and $Pb^{2+}$ (6) (*SI Text*). Of these heavy metal ions, CS3 does show some turn-on response to $Ag^+$ at high, nonphysiological levels, but the addition of $Cu^+$ reveals that $Cu^+$ can displace $Ag^+$ from the sensor. The large fluorescent turn-on response of CS3 to $Cu^+$, in conjunction with its high selectivity in the presence of interfering ions, suggests that this tool is a promising reagent for imaging basal levels of exchangeable $Cu^+$ pools in living cells.

**CS3 Is Capable of Imaging Labile Pools of Copper in Living Cells at Basal and Copper-Depleted Levels.** The two previously reported turn-on small-molecule fluorescent probes for live-cell $Cu^+$ detection, CTAP-1 and CS1, are capable of detecting changes in labile intracellular copper levels, but their relatively low quantum efficiencies limit their use to visualizing differences under situations of acute or prolonged copper overload (29, 30). We reasoned that CS3, with its improved brightness and turn-on response to $Cu^+$, would provide the ability to report pools of intracellular, exchangeable $Cu^+$ at basal levels. We therefore sought to test whether this chemical tool could image labile copper stores under both basal and copper-depleted conditions. To this end we depleted cells of their endogenous copper stores by culturing them in media containing the membrane-impermeable chelator bathocuproine disulfonate (BCS). This treatment has been shown to mildly decrease copper levels within mammalian cells without compromising their viability (36). Accordingly, human embryonic kidney (HEK 293T) cells were grown either in normal media or in media containing 200 μM BCS for 20 h to make them copper depleted, stained with 2 μM CS3 for 10 min, and subsequently imaged by confocal microscopy (Fig. 3). Cells grown in normal control media exhibit markedly higher fluorescence signals compared to cells grown in the presence of BCS (Fig. 3 *A* and *B*), indicating that CS3 can respond to changes in basal, endogenous levels of exchangeable $Cu^+$ as well as sense differences between copper-depleted and copper-normal conditions. To provide further support that BCS targets copper selectively, we treated HEK 293T cells with BCS and then stained them with the $Zn^{2+}$-responsive dye FluoZin-3 AM. We find that the zinc levels as measured by the zinc probe are not statistically different in the BCS-treated cells relative to the control (*SI Text*). In addition, we treated HEK 293T cells with BCS and imaged total metal pools by XRFM. We find that copper levels are significantly decreased in BCS-treated cells relative to control cells, whereas phosphorus and zinc show the opposite trend (*SI Text*).

We also examined whether CS3 could report more acute changes in exchangeable intracellular copper pools by treating cells with 100 μM of the competing cell-permeable $Cu^+$-chelator tris((ethylthio)ethylamine) (TEMEA) and CS3 for 10 min. (Fig. 3*C*). The observed fluorescence signal was muted upon introduction of this competing copper ligand, indicating that CS3 responds reversibly to $Cu^+$ and can sense dynamic variations in kinetically labile $Cu^+$ pools in living mammalian cells. In addition, nuclear staining with Hoechst 33342 affirms that the viability of HEK 293T cells is not affected by CS3 staining or the manipulation of cellular copper status.

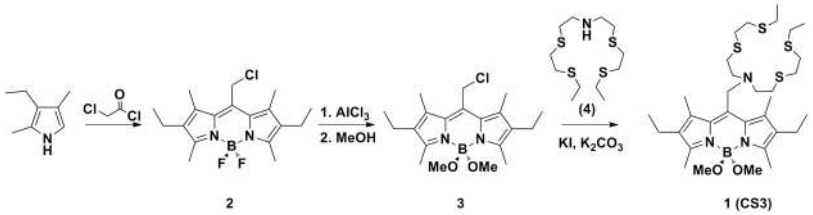


**Fig. 1.** Synthesis of CS3.

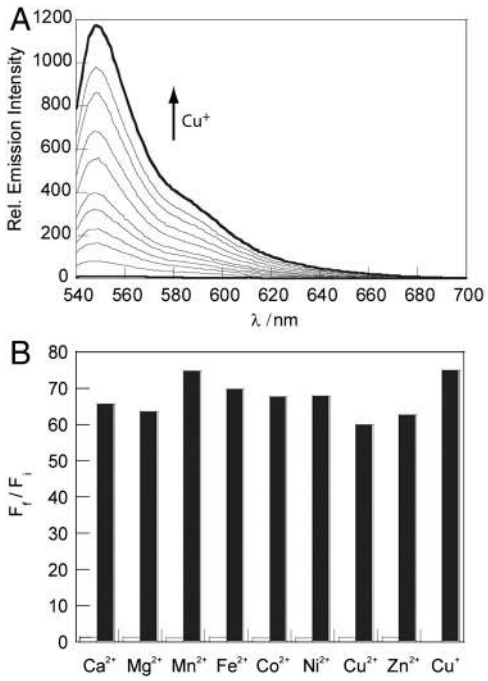


**Fig. 2.** Spectroscopic responses and selectivity of CS3. All spectra were acquired in 20 mM HEPES, pH 7, at 25 °C. (*A*) Fluorescence response of 4 μM CS3 to $Cu^{+}$. Spectra shown are for buffered [$Cu^{+}$] of 0, 0.3, 0.5, 0.8, 1.0, 1.5, 2.0, 2.5, 3.0, 3.5, and 4.0 μM. (*B*) Fluorescence responses of CS3 to various metal ions. Bars represent the final integrated fluorescence response ($F_f$) over the initial integrated emission ($F_i$). White bars represent the addition of an excess of the appropriate metal ion (2 mM for $Ca^{2+}$, $Mg^{2+}$, and $Zn^{2+}$; 50 μM for all other cations) to a 4 μM solution of CS3. Black bars represent the subsequent addition of 4 μM $Cu^{+}$ to the solution. Excitation was provided at 530 nm, and the collected emission was integrated over 540 to 700 nm.

**Discovery of Depolarization-Induced Movements of Copper Pools in Neurons with Live-Cell CS3 Molecular Imaging.** With data showing that CS3 is capable of reporting dynamic changes in endogenous intracellular $Cu^{+}$ stores by molecular imaging and that this probe is sensitive enough to visualize labile pools under basal conditions, we then sought to use this chemical tool to probe copper homeostasis in brain neurons. To this end, live hippocampal dissociated cultured neurons stained with 2 μM CS3 show a diffuse fluorescent signal pattern, localized mainly in the soma (Fig. 4*A*). To evaluate the spatial distributions of labile $Cu^{+}$ pools in these neuronal cells under basal conditions, we measured the emission intensity ratio of dendritic copper to somatic copper regions ($D_{Cu}:S_{Cu}$). Quantification of the dendritic and somatic fluorescence intensity signals provides a $D_{Cu}:S_{Cu}$ ratio signal of $0.24 \pm 0.04$ in these resting neurons.

We then moved on to characterize the distribution of labile copper pools in activated neuronal cells. Interestingly, we observed that neurons treated with 50 mM KCl for 2 min to induce their depolarization and stained with 2 μM CS3 show a marked redistribution of labile copper pools from their somatic cell bodies to peripheral processes, quantified by a patent increase in $D_{Cu}:S_{Cu}$ ratio to $0.35 \pm 0.04$ (Fig. 4*E*). These imaging data, which provide direct evidence that the spatial distributions of copper change upon neuronal activation, suggest that the redistribution of labile copper pools might be a result of a rise in dendritic levels and/or a decrease in somatic levels.

**XRFM Provides an Independent and Complementary Method for Visualizing Mobile Copper Triggered in Depolarized Neuronal Cells.** To study mobile copper in neuronal cells using an independent technique as well as verify our CS3-based molecular imaging results, we performed XRFM experiments at the Advanced Photon Source of the Argonne National Laboratory. XRFM affords, without any added reagents, a direct method for measuring total copper and other element distributions by their synchotron-induced X-ray fluorescence signatures (29, 37–40). In particular, the instrument at the 2-ID-E beamline at the Advanced Photon Source of the Argonne National Laboratory boasts a spatial resolution of 200 nm, which makes it appropriate for examining the subcellular elemental distributions of single cells (41). We emphasize that the XRFM method measures total element content on fixed samples, thus providing a complementary approach to live-cell imaging of labile metal pools using fluorescent sensors. Moreover, the combination of small-molecule fluorescence imaging and XRFM has been exploited previously to provide a coherent picture of copper homeostasis in resting mammalian cells, setting the stage for studies of copper homeostasis in dynamic and stimulated situations in the present study (26, 27).

For the XRFM experiments, we utilized the same types of hippocampal neurons employed for the live-cell CS3 imaging studies but cultured on silicon nitride windows. These neuronal cell cultures were incubated either in buffer for 2 min as a baseline control or in buffer supplemented with 50 mM KCl to trigger their depolarization. The cells were then promptly fixed with paraformaldehyde (PFA) and examined by XRFM (Fig. 4). The elemental maps of total copper, zinc, and phosphorus pools are shown for baseline control neurons treated with buffer prior to fixation (Fig. 4 *B*–*D*). Phosphorus and zinc signals are concen-

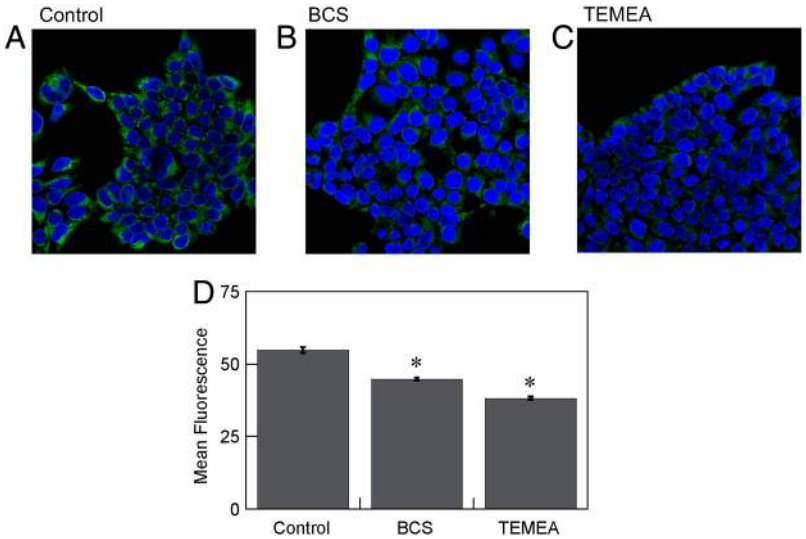


**Fig. 3.** Molecular imaging of endogenous basal Cu in HEK 293T cells with CS3. (*A*) Control HEK 293T cells, (*B*) HEK 293T cells supplemented with 200 μM BCS in the growth medium for 20 h at 37 °C, and (*C*) HEK 293T cells treated with 100 μM TEMEA for 10 min. *A*, *B*, and *C* were stained with 2 μM CS3, 5 μM Hoechst 33342, and DMSO vehicle for TEMEA for 10 min at 37 °C in DMEM. (*D*) Graph showing the quantification of mean fluorescence intensity of each condition normalized to the control condition ($n = 5$ fields of cells per condition). Error bars represent the SEM. Asterisk (*) indicates $P < 0.01$ compared to control cells.

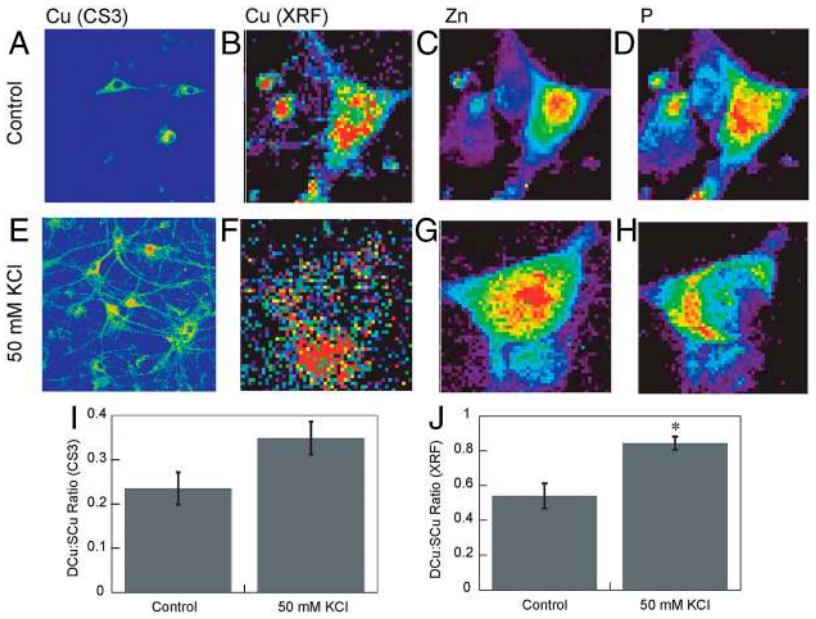


**Fig. 4.** Molecular imaging of Cu distributions in resting and depolarized rat hippocampal neurons with CS3 and XRFM. (*A*) Live primary rat hippocampal neurons treated with extracellular solution (ECS) buffer for 2 min and then stained with 2 μM CS3 for 10 min. (*B–D*) Rat hippocampal neurons treated with ECS buffer for 2 min, fixed with 4% PFA and imaged by XRFM. Images shown are for (*B*) Cu, (*C*) Zn, and (*D*) P channels. (*E*) Live primary rat hippocampal neurons treated with 50 mM KCl in ECS buffer for 2 min and then stained with 2 μM CS3 for 10 min. (*F–H*) Rat hippocampal neurons treated with 50 mM KCl in ECS buffer for 2 min and then fixed with 4% PFA and imaged by XRFM. Images shown are for (*F*) Cu, (*G*) Zn, and (*H*) P channels. (*I*) Graph showing the blinded quantification of CS3-derived dendrite:soma fluorescence ratios for resting and depolarized neurons ($n = 18$). Error bars represent SEM ($P = 0.09$). (*J*) Graph showing the XRF dendrite:soma fluorescence ratios for resting and depolarized neurons. Error bars represent SEM. Asterisk (*) indicates $P < 0.05$.

trated in the nuclear region, whereas copper maintains a perinuclear distribution pattern located primarily in the somatic cell body, consistent with the results obtained from the live-cell CS3 imaging studies. Also in line with the CS3 imaging data, neurons depolarized with 50 mM KCl show a significant change in cellular copper signal that is more diffuse in the depolarized brain cells compared to resting ones (Fig. 4 *F–H*), with copper pools displaying a marked redistribution from the cell body to peripheral processes. In contrast to the copper channel, similar elemental distributions of phosphorus and zinc are observed in the KCl-depolarized neurons compared to their unstimulated counterparts, revealing the relative mobility of copper pools in this model under these conditions. Quantification of the dendritic:somatic copper ratio from XRFM data collected from multiple Advanced Photon Source beam runs over 4 y shows a statistically significant increase in KCl-stimulated neurons ($0.84 \pm 0.04$) compared to basal, untreated neurons ($0.54 \pm 0.07$) (Fig. 4*J*). Taken together, the CS3 and XRFM imaging experiments provide two independent methods that have allowed us to discover and establish that brain neurons trigger movements of intracellular copper pools upon their activation, causing a significant redistribution of neuronal copper stores from their somatic cell bodies to peripheral processes.

**CS3 Imaging and XRFM Show that Cellular Copper Movements are Dependent on Calcium Release.** We next used CS3-based molecular imaging and XFRM to probe the effects of intracellular calcium release, a primary consequence of depolarization-induced neural activity, on the observed cellular copper movements. Multiple and distinct types of treatments to alter calcium release, including direct metal chelation or inhibition of cellular calcium entry channels or intracellular receptors, support a relationship between mobile copper and calcium signaling in this model.

First, intracellular calcium rises in neurons were blocked by treatment with the established intracellular $Ca^{2+}$ chelator BAPTA, delivered in its membrane-permeable acetoxymethyl form BAPTA-AM; this prochelator undergoes rapid hydrolysis by intracellular esterases to produce BAPTA (42). As shown in Fig. 5, $Ca^{2+}$ chelation prevents KCl-induced redistribution of neuronal copper pools, as the observed $D_{Cu} : S_{Cu}$ ratio in BAPTA-AM–trea-

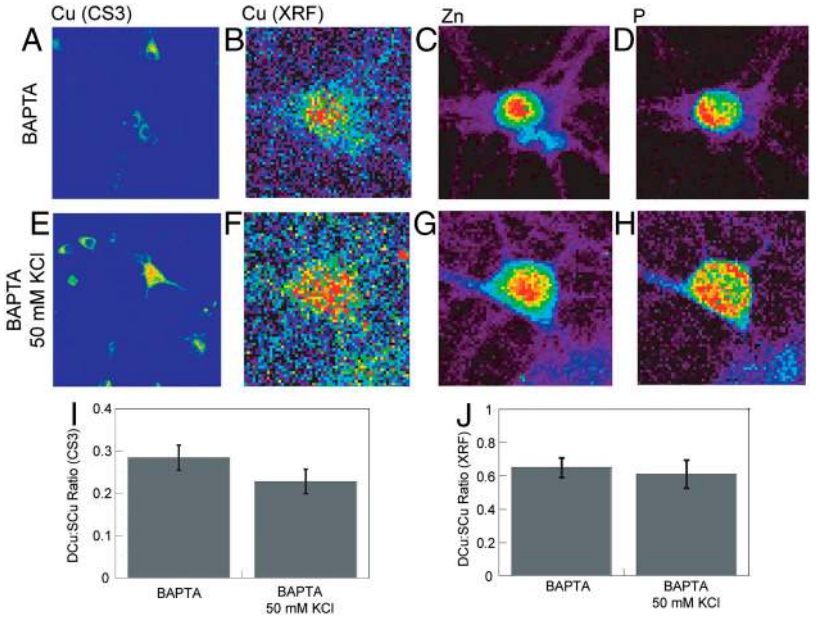


**Fig. 5.** (*A*) Rat hippocampal neurons treated with ECS buffer for 2 min with 10 μM BAPTA-AM and then stained with 2 μM CS3 for 10 min. (*B–D*) Rat hippocampal neurons treated with ECS buffer with 10 μM BAPTA-AM for 2 min and then fixed with 4% PFA and imaged by XRFM. Images shown are for (*B*) Cu, (*C*) Zn, and (*D*) P channels. (*E*) Live primary rat hippocampal neurons treated with 50 mM KCl in ECS buffer with 10 μM BAPTA-AM for 2 min and then stained with 2 μM CS3 for 10 min. (*F–H*) Rat hippocampal neurons treated with 50 mM KCl in ECS buffer with 10 μM BAPTA-AM for 2 min and then fixed with 4% PFA and imaged by XRFM. Images shown are for (*F*) Cu, (*G*) Zn and (*H*) P channels. (*I*) Graph showing the blinded quantification of CS3-derived dendrite:soma fluorescence ratios for BAPTA-AM–treated ($n = 22$) and BAPTA-AM/KCl–treated ($n = 16$) neurons. Error bars represent SEM. (*J*) Graph showing the XRF dendrite:soma fluorescence ratios for resting and depolarized BAPTA-AM–treated neurons. Error bars represent SEM.

ted, KCl-depolarized neurons is similar to unstimulated samples as measured by CS imaging. The collective data provide evidence that transient elevation of intracellular calcium levels is required upstream of depolarization-induced copper translocation and provide a link between mobile copper and calcium, a major modulator of cell signaling pathways.

We then performed XRFM experiments to independently establish that calcium signaling is required to trigger activity-dependent copper movements in these neuronal cell models. Neurons were pretreated with BAPTA-AM and either mock treated with BAPTA-AM–containing buffer for 2 min or with buffer containing 50 mM KCl and 10 μM BAPTA-AM. Notably, the XRFM images directly show that the levels and distributions of cellular copper are not perturbed by BAPTA treatment. Moreover, XRFM analysis of these cells indicated no significant differences in copper distributions between cells that had been treated with only buffer (Fig. 5 *B–D*) or cells that had been depolarized (Fig. 5 *F–H*). These results, in conjunction with the CS3 imaging of live neurons, reinforce the link between calcium signaling and mobile copper pools in brain cell systems.

In further support of the aforementioned experiments, we then proceeded to alter calcium signaling pathways using reagents that are not metal chelators. First, we added dantrolene, a well-established drug that decreases intracellular calcium levels by binding to the ryanodine receptor (43, 44). As shown in Fig. 6, dantrolene also blocks KCl-induced redistribution of neuronal copper pools, as the observed $D_{Cu}:S_{Cu}$ ratio in dantrolene-treated, KCl-depolarized neurons is similar to unstimulated samples as monitored by CS imaging. Next, we added nifedipine, a classic dihydropyridine calcium channel blocker that inhibits transmembrane flux of extracellular calcium ions (44). Unlike the dantrolene and BAPTA treatments, nifedipine at this dose does not diminish the KCl-induced mobilization of labile copper pools to the same extent. Finally, the combined application of both dantrolene and nifedipine also abolishes the depolarization-triggered soma-to-dendrite movements of neuronal copper. By showing that interfering with calcium entry or intracellular receptor pathways can also block depolarization-induced movements of neuronal copper, these additional lines of evidence provide further support for a link between mobile copper and calcium signaling.

## Concluding Remarks

Dynamic metal fluxes triggered by physiological stimulation are well established for alkali and alkaline earth metals like potassium, sodium, and calcium in a wide range of cell types but are insufficiently explored for transition metals. In this work, we utilize a fluorescent sensor and XRFM imaging to directly show that movements of copper pools are triggered by cell activation in a neuronal model, suggesting that this transition metal nutrient can also participate as a dynamic component for essential physiological functions. Indeed, cellular copper uptake and release is kinetically rapid (45), and growing evidence highlights the importance of orchestrating transient copper accumulation, compartmentalization, and efflux events within subcellular compartments at a molecular level (13, 28, 46–51). The brain's high copper demand, along with growing connections between copper misregulation and neurodegenerative diseases, point to the particular importance of understanding copper homeostasis in this unique biological system.

In this report, we have presented CS3, a fluorescent sensor where improvements in turn-on response and quantum efficiency give this probe a unique ability to monitor labile copper pools in living cells at basal and copper-depleted conditions. We have used this chemical probe in conjunction with XRFM in a combined imaging study to discover that neuronal cells move significant pools of copper from their somatic cell bodies to extended outer processes when activated by depolarization. Moreover, additional CS3 and XRFM imaging experiments establish that the observed copper redistributions are dependent on calcium release, showing that mobile copper is linked to a major hub of cell signaling pathways and presages a wide range of possibilities for exploring copper and calcium crosstalk.

The ability to directly monitor mobile pools of copper during different stages of neuronal cell activity highlights the combined use of live-cell molecular imaging for visualizing exchangeable copper pools along with XRFM to characterize total copper content as a synergistic approach to study metal homeostasis

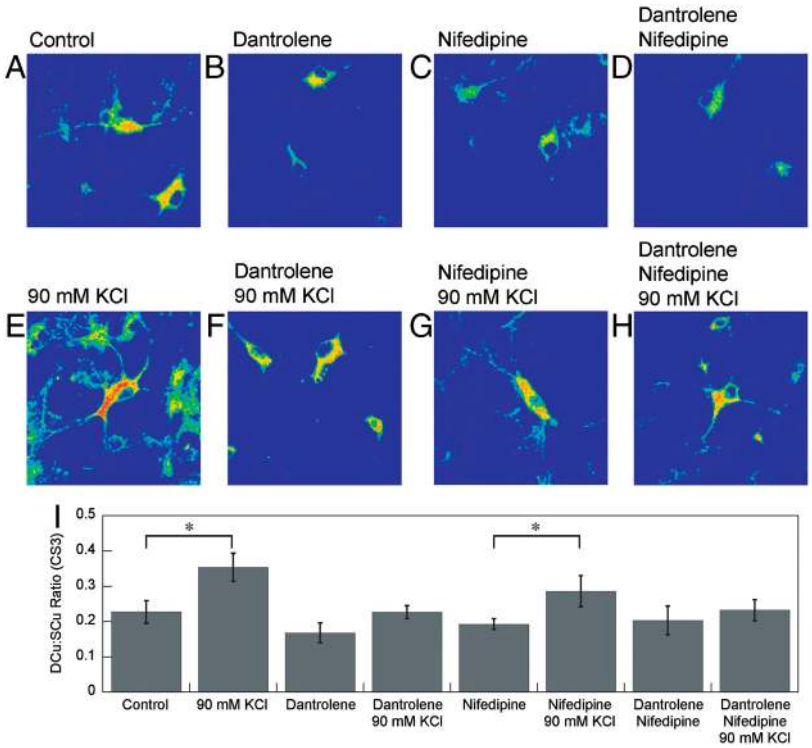


**Fig. 6.** Molecular imaging of Cu distributions in resting, depolarized, and inhibitor-treated rat hippocampal neurons with CS3. (*A*) Live primary rat hippocampal neurons treated with ECS buffer for 10 min, (*B*) treated with ECS buffer with 30 μM dantrolene for 10 min, (*C*) treated with ECS buffer with 100 μM nifedipine for 10 min, (*D*) treated with ECS buffer with 30 μM dantrolene and 100 μM nifedipine for 10 min, (*E*) treated with 90 mM KCl in ECS buffer for 2 min, (*F*) treated with 30 μM dantrolene in ECS buffer for 10 min and then 90 mM KCl in ECS buffer for 2 min, (*G*) treated with 100 μM nifedipine in ECS buffer for 10 min and then 90 mM KCl in ECS buffer for 2 min, and (*H*) treated with 30 μM nifedipine and 100 μM dantrolene in ECS buffer for 10 min and then 90 mM KCl in ECS buffer for 2 min and then stained with 2 μM CS3 for 10 min. (*I*) Graph showing the blinded quantification of CS3-derived dendrite:soma fluorescence ratios for resting, depolarized, and inhibitor-treated neurons ($n \geq 11$). Error bars represent the SEM. Asterisk (*) indicates $P < 0.05$.

in a native cellular context. Our findings, taken together with previous reports showing accumulation of mitochondria to neuronal filopodia and dendritic spines upon repeated depolarization (52), reversible trafficking of the P-type ATPase ATP7A from the perinuclear trans-Golgi to neuronal processes by NMDA receptor activation (23), and axonal localization of ATP7A potentially involved in process guidance (53, 54), point to the intriguing possibility that subcellular compartmentalization and transient reorganization of copper stores is essential to tuning dynamic neuronal activity. Furthermore, the requirement for calcium release to trigger copper movements provides an entry for connecting copper to canonical signal transduction pathways. We are actively pursuing an understanding of mobile copper as a potential new metal signal in the context of neuronal activity and other fundamental physiological processes.

**ACKNOWLEDGMENTS.** We thank Orapim Tulyathan and Prof. Ehud Isacoff for providing neuronal cultures for preliminary survey studies, and Dr. Bryan Dickinson and Dr. Elizabeth New for help with one of the XRFM experiments. We thank the Packard and Sloan Foundations; the University of California, Berkeley Hellman Faculty Fund; Amgen; Astra Zeneca; Novartis; and the National Institutes of Health (GM 79465) for providing funding for this work. C.J.C. is an Investigator with the Howard Hughes Medical Institute. D.W.D. and E.W.M. were partially supported by a Chemical Biology Training Grant from the National Institutes of Health (T32 GM066698), and E.W.M. acknowledges a Stauffer graduate fellowship. Confocal fluorescence images were acquired at the Molecular Imaging Center at University of California, Berkeley. Work at the Advanced Photon Source was supported by the Department of Energy, Office of Science Contract DE-AC-02-06CH11357.

1. Tsien RW, Tsien RY (1990) Calcium channels, stores, and oscillations. *Annu Rev Cell Biol* 6:715–760.
2. Debanne D (2004) Information processing in the axon. *Nat Rev Neurosci* 5:304–316.
3. Clapham DE (2007) Calcium signaling. *Cell* 131:1047–1058.
4. Lippard SJ, Berg JM (1994) *Principles of Bioinorganic Chemistry* (University Science Books, Mill Valley, CA).
5. Gray HB, Stiefel EI, Valentine JS, Bertini I (2007) *Biological Inorganic Chemistry* (University Science Books, Mill Valley, CA).
6. Cvetkovic A, et al. (2010) Microbial metalloproteomes are largely uncharacterized. *Nature* 466:779–782.
7. Berridge MJ, Bootman MD, Lipp P (1998) Calcium—A life and death signal. *Nature* 395:645–648.
8. Atwood CS, et al. (1999) *Metal Ions in Biological Systems: Interrelations Betwen Free Radicals and Metal Ions in Life Processes* (CRC, New York).
9. Bush AI (2000) Metals and neuroscience. *Curr Opin Chem Biol* 4:184–191.
10. Burdette SC, Lippard SJ (2003) Bioinorganic Chemistry Special Feature: Meeting of the minds: Metalloneurochemistry. *Proc Natl Acad Sci USA* 100:3605–3610.
11. Prohaska JR, Gybina AA (2004) Intracellular copper transport in mammals. *J Nutr* 134:1003–1006.
12. Que EL, Domaille DW, Chang CJ (2008) Metals in neurobiology: Probing their chemistry and biology with molecular imaging. *Chem Rev* 108:1517–1549.
13. Camakaris J, Voskoboinik I, Mercer JF (1999) Molecular mechanisms of copper homeostasis. *Biochem Biophys Res Commun* 261:225–232.
14. Bertini I, Rosato A (2008) Menkes disease. *Cell Mol Life Sci* 65:89–91.
15. Barnham KJ, Masters CL, Bush AI (2004) Neurodegenerative diseases and oxidative stress. *Nat Rev Drug Discov* 3:205–214.
16. Gaggelli E, Kozlowski H, Valensin D, Valensin G (2006) Copper homeostasis and neurodegenerative disorders (Alzheimer's, prion, and Parkinson's diseases and amyotrophic lateral sclerosis). *Chem Rev* 106:1995–2044.
17. Lutsenko S, Gupta A, Burkhead JL, Zuzel V (2008) Cellular multitasking: The dual role of human Cu-ATPases in cofactor delivery and intracellular copper balance. *Arch Biochem Biophys* 476:22–32.
18. Beckman JS, Estevez AG, Crow JP, Barbeito L (2001) Superoxide dismutase and the death of motoneurons in ALS. *Trends Neurosci* 24:S15–S20.
19. Valentine JS, Hart PJ (2003) Bioinorganic Chemistry Special Feature: Misfolded CuZn-SOD and amyotrophic lateral sclerosis. *Proc Natl Acad Sci USA* 100:3617–3622.
20. Brown DR, Kozlowski H (2004) Biological inorganic and bioinorganic chemistry of neurodegeneration based on prion and Alzheimer diseases. *Dalton Trans* 1907–1917.
21. Millhauser GL (2004) Copper binding in the prion protein. *Acc Chem Res* 37:79–85.
22. Hartter DE, Barnea A (1988) Evidence for release of copper in the brain: Depolarization-induced release of newly taken up copper. *Synapse* 2:412–415.
23. Schlief ML, Craig AM, Gitlin JD (2005) NMDA receptor activation mediates copper homeostasis in hippocampal neurons. *J Neurosci* 25:239–246.
24. Hopt A, et al. (2003) Methods for studying synaptosomal copper release. *J Neurosci Methods* 128:159–172.
25. Schlief ML, et al. (2006) Role of the Menkes copper-transporting ATPase in NMDA receptor-mediated neuronal toxicity. *Proc Natl Acad Sci USA* 103:14919–14924.
26. Domaille DW, Que EL, Chang CJ (2008) Synthetic fluorescent sensors for studying the cell biology of metals. *Nat Chem Biol* 4:168–175.
27. McRae R, Bagchi P, Sumalekshmy S, Fahrni CJ (2009) In situ imaging of metals in cells and tissues. *Chem Rev* 109:4780–4827.
28. Haas KL, Franz KJ (2009) Application of metal coordination chemistry to explore and manipulate cell biology. *Chem Rev* 109:4921–4960.
29. Yang LC (2005) Imaging of the intracellular topography of copper with a fluorescent sensor and by synchrotron x-ray fluorescence microscopy. *Proc Natl Acad Sci USA* 102:11179–11184.
30. Zeng L, et al. (2006) A selective turn-on fluorescent sensor for imaging copper in living cells. *J Am Chem Soc* 128:10–11.
31. Miller EW, Zeng L, Domaille DW, Chang CJ (2006) Preparation and use of Coppersensor-1, a synthetic fluorophore for live-cell copper imaging. *Nat Protoc* 1:824–827.
32. Domaille DW, Zeng L, Chang CJ (2010) Visualizing ascorbate-triggered release of labile copper within living cells using a ratiometric fluorescent sensor. *J Am Chem Soc* 132:1194–1195.
33. Wegner SV, et al. (2010) Dynamic copper(I) imaging in mammalian cells with a genetically encoded fluorescent copper(I) sensor. *J Am Chem Soc* 132:2567–2569.
34. Wegner SV, Sun F, Hernandez N, He C (2011) The tightly regulated copper window in yeast. *Chem Commun* 47:2571–2573.
35. Gabe Y (2006) Tunable design strategy for fluorescence probes based on 4-substituted BODIPY chromophore: Improvement of highly sensitive fluorescence probe for nitric oxide. *Anal Bioanal Chem* 386:621–626.
36. Hamza I, Prohaska J, Gitlin JD (2003) Essential role for Atox1 in the copper-mediated intracellular trafficking of the Menkes ATPase. *Proc Natl Acad Sci USA* 100:1215–1220.
37. Glesne D, et al. (2006) Regulatory properties and cellular redistribution of zinc during macrophage differentiation of human leukemia cells. *J Struct Biol* 155:2–11.
38. Finney L, et al. (2007) X-ray fluorescencemicroscopy reveals large-scale relocalization and extracellular translocation of cellular copper during angiogenesis. *Proc Natl Acad Sci USA* 104:2247–2252.
39. Fahrni CJ (2007) Biological applications of X-ray fluorescence microscopy: Exploring the subcellular topography and speciation of transition metals. *Curr Opin Chem Biol* 11:121–127.
40. Finney L, et al. (2010) Imaging metals in proteins by combining electrophoresis with rapid X-ray fluorescence mapping. *ACS Chem Biol* 5:577–587.
41. Twining BS, et al. (2003) Quantifying trace elements in individual aquatic protist cells with a synchrotron X-ray fluorescence microprobe. *Anal Chem* 75:3806–3816.
42. Tsien RY (1980) A non-disruptive technique for loading calcium buffers and indicators into cells. *Nature* 290:527–528.
43. Balkowiec A, Katz DM (2002) Cellular mechanisms regulating activity-dependent release of native brain-derived neurotrophic factor from hippocampal neurons. *J Neurosci* 22:10399–10407.
44. Hayashi T, et al. (1997) Effect of dantrolene on KCl- or NMDA-induced intracellular $Ca^{2+}$ changes and spontaneous $Ca^{2+}$ oscillation in cultured rat frontal cortical neurons. *J Neural Transm* 104:811–824.
45. Herd SM (1987) Uptake and efflux of copper-64 in Menkes'-disease and normal continuous lymphoid cell lines. *Biochem J* 247:341–347.
46. O'Halloran TV, Culotta VC (2000) Metallochaperones, an intracellular shuttle service for metal ions. *J Biol Chem* 275:25057–25060.
47. Rosenzweig AC, O'Halloran TV (2000) Structure and chemistry of the copper chaperone proteins. *Curr Opin Chem Biol* 4:140–147.
48. Cobine PA, Pierrel F, Winge DR (2006) Copper trafficking to the mitochondrion and assembly of copper metalloenzymes. *Biochim Biophys Acta* 1763:759–772.
49. Kim B-E, Nevitt T, Thiele DJ (2008) Mechanisms for copper acquisition, distribution and regulation. *Nat Chem Biol* 4:176–185.
50. Davis AV, O'Halloran TV (2008) A place for thioether chemistry in cellular copper ion recognition and trafficking. *Nat Chem Biol* 4:148–151.
51. Ma Z, Jacobsen FE, Giedroc DP (2009) Coordination chemistry of bacterial metal transport and sensing. *Chem Rev* 109:4644–4681.
52. Li Z, Okamoto K-I, Hayashi Y, Sheng M (2004) The importance of dendritic mitochondria in the morphogenesis and plasticity of spines and synapses. *Cell* 119:873–887.
53. El Meskini R, Cline LB, Eipper BA, Ronnett GV (2005) The developmentally regulated expression of Menkes protein ATP7A suggests a role in axon extension and synaptogenesis. *Dev Neurosci Basel* 27:333–348.
54. El Meskini R, et al. (2007) ATP7A (Menkes protein) functions in axonal targeting and synaptogenesis. *Mol Cell Neurosci* 34:409–421.